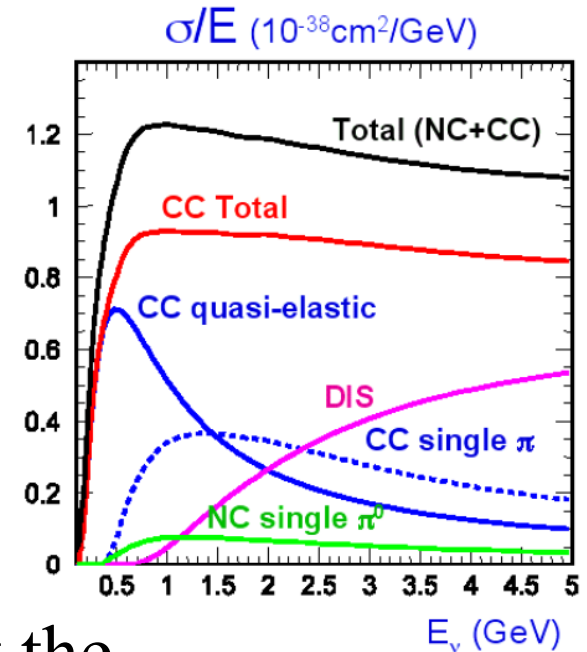


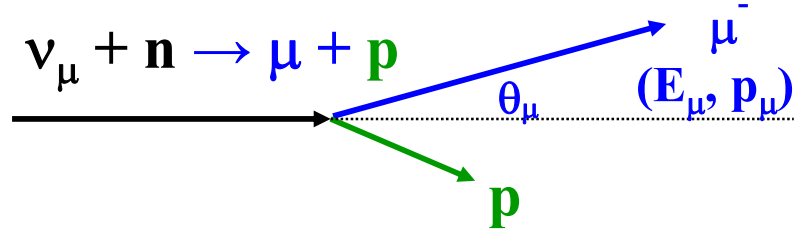
3. Cross Sections of ~GeV neutrinos

- It is the energy of accelerator neutrinos for the long baseline.
- Dominant Interaction Mode
 - Elastic scattering.
 - CC: Quasi-elastic scattering.
 - NC: Elastic scattering.
 - 1π production with hadron resonance.
 - 1π production in coherent scattering.
 - Deep inelastic scattering.
- Not only the baseline interaction, but the secondary interaction in the nucleus makes the story difficult
 - Tutorial by J. Morfin?



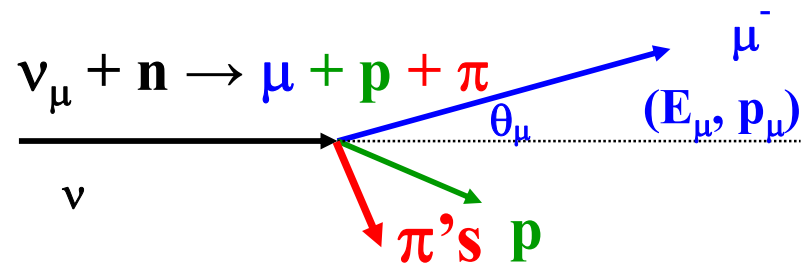
K2K Neutrino Energy E_ν Reconstruction

CC quasi elastic (QE)

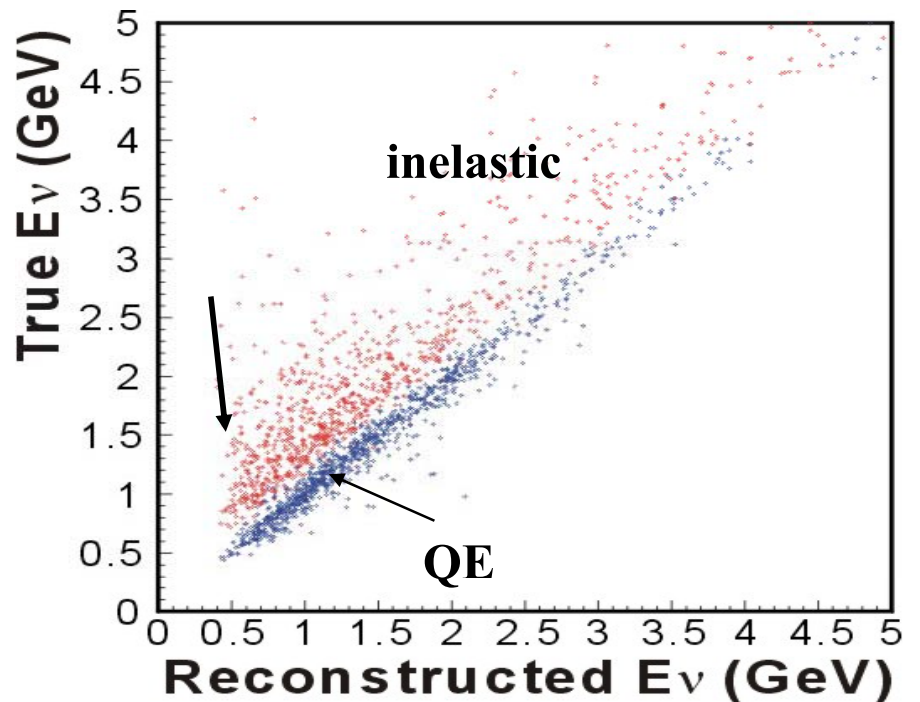


$$E_\nu = \frac{m_N E_\mu - m_\mu^2 / 2}{m_N - E_\mu + \mathbf{p}_\mu \cos \theta_\mu}$$

CC inelastic

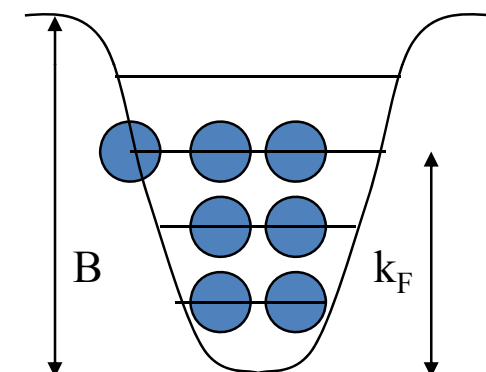
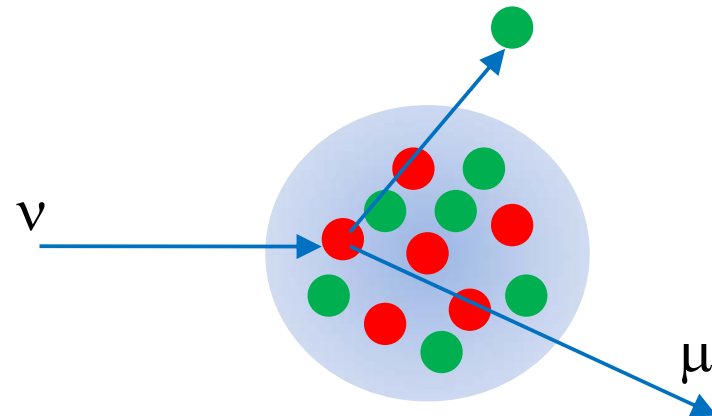


Rate($E\nu$,Near) $\rightarrow \phi(E\nu$,Near)
 \uparrow
 $\sigma(\text{QE}), \sigma(\text{nonQE})$

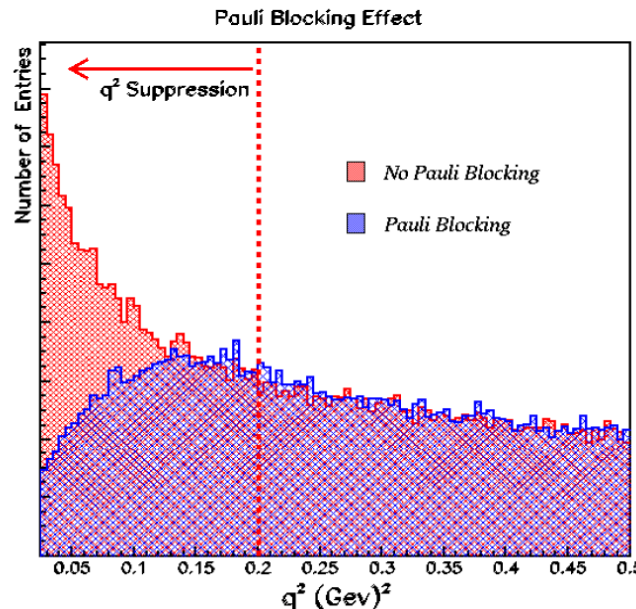


CC Quasi-elastic scattering with nucleus

- A Fermi gas model
 - The interaction take place through quasi-free scattering of nucleons contained in the non-interacting Fermi gas.



- Nucleons in the initial state have momentum (Fermi momentum) $\sim 200\text{MeV}/c$
- The nucleon in the final state must have the momentum above Fermi momentum surface.
 - Pauli blocking \Rightarrow low Q2 suppression.



- We must take into account of the form factors of a nucleon.

$$F_V(Q^2 = -q^2) = \frac{1}{\left(1 + \frac{Q^2}{M_V^2}\right)^2}$$

$$F_A(Q^2) = \frac{1}{\left(1 + \frac{Q^2}{M_A^2}\right)^2}$$

$$\begin{aligned} \frac{d\sigma}{dQ^2} &= \frac{G^2 \cos^2 \theta_C}{4\pi} \{(F_V + F_W + F_A)^2 + (F_V + F_W + F_A)^2 \left(1 - \frac{Q^2}{2E_\nu m_N}\right)^2 \\ &+ [F_A^2 - (F_V + F_W)^2] \frac{Q^2}{2E_\nu^2} \\ &+ \left[F_W^2 \frac{(Q^2 + 4m_N^2)}{4m_N^2} - 2(F_V + F_W)F_W\right] \left[2 - \frac{Q^2(m_N + 2E_\nu)}{2E_\nu^2 m_N}\right]\} \end{aligned}$$

$$F_W(Q^2) \propto F_V(Q^2)$$

F_W : Weak magnetism tensor term

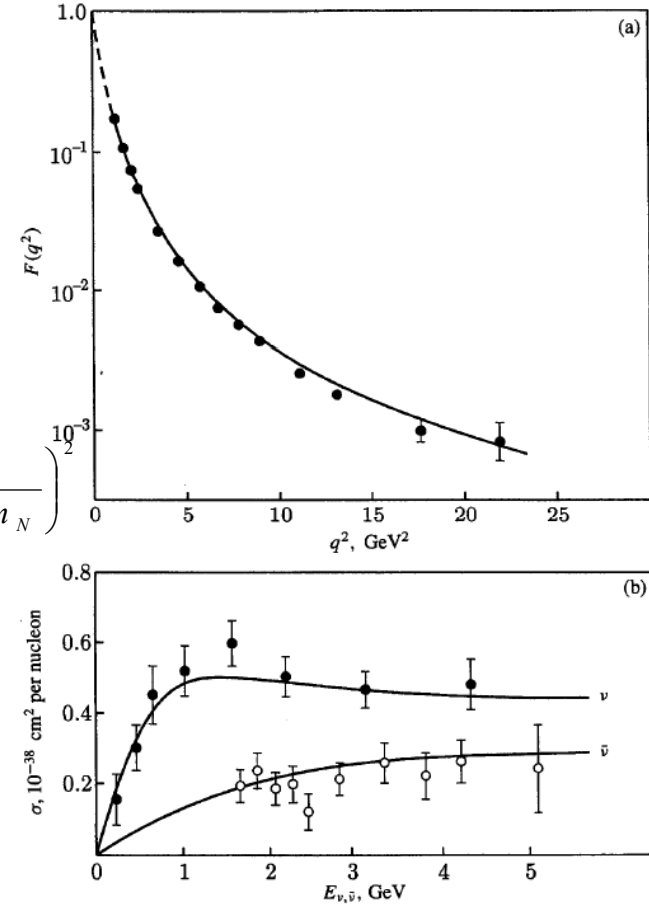
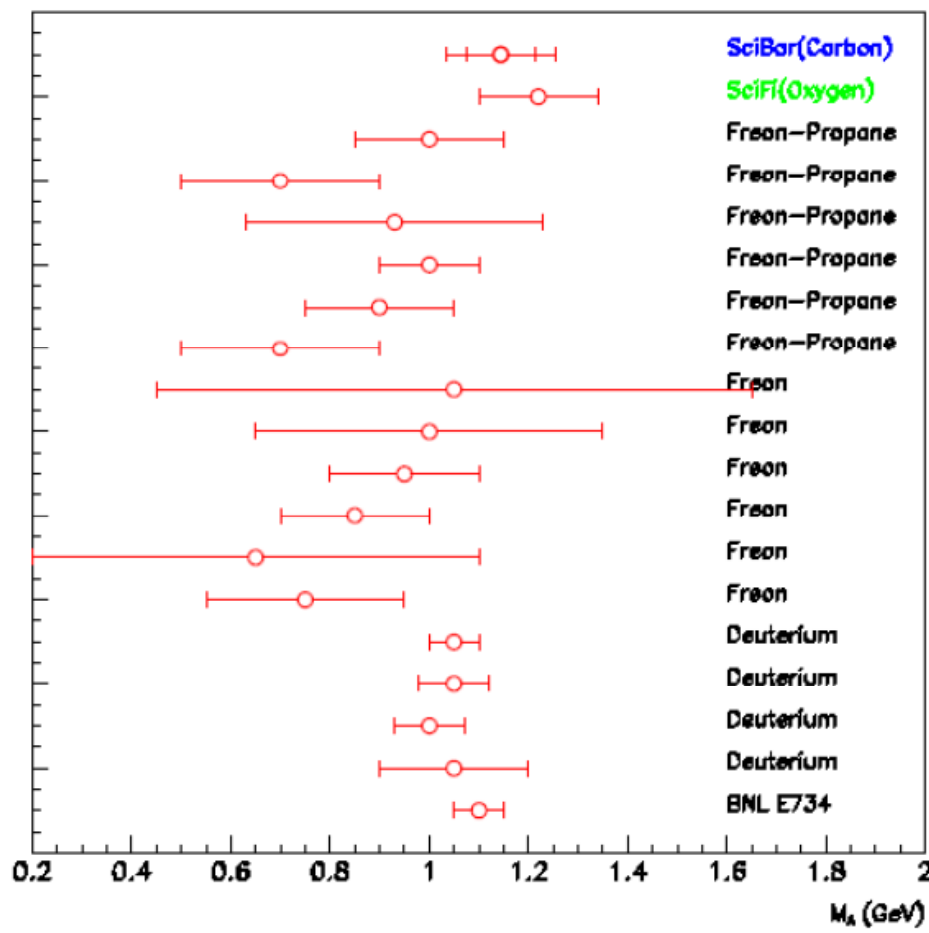


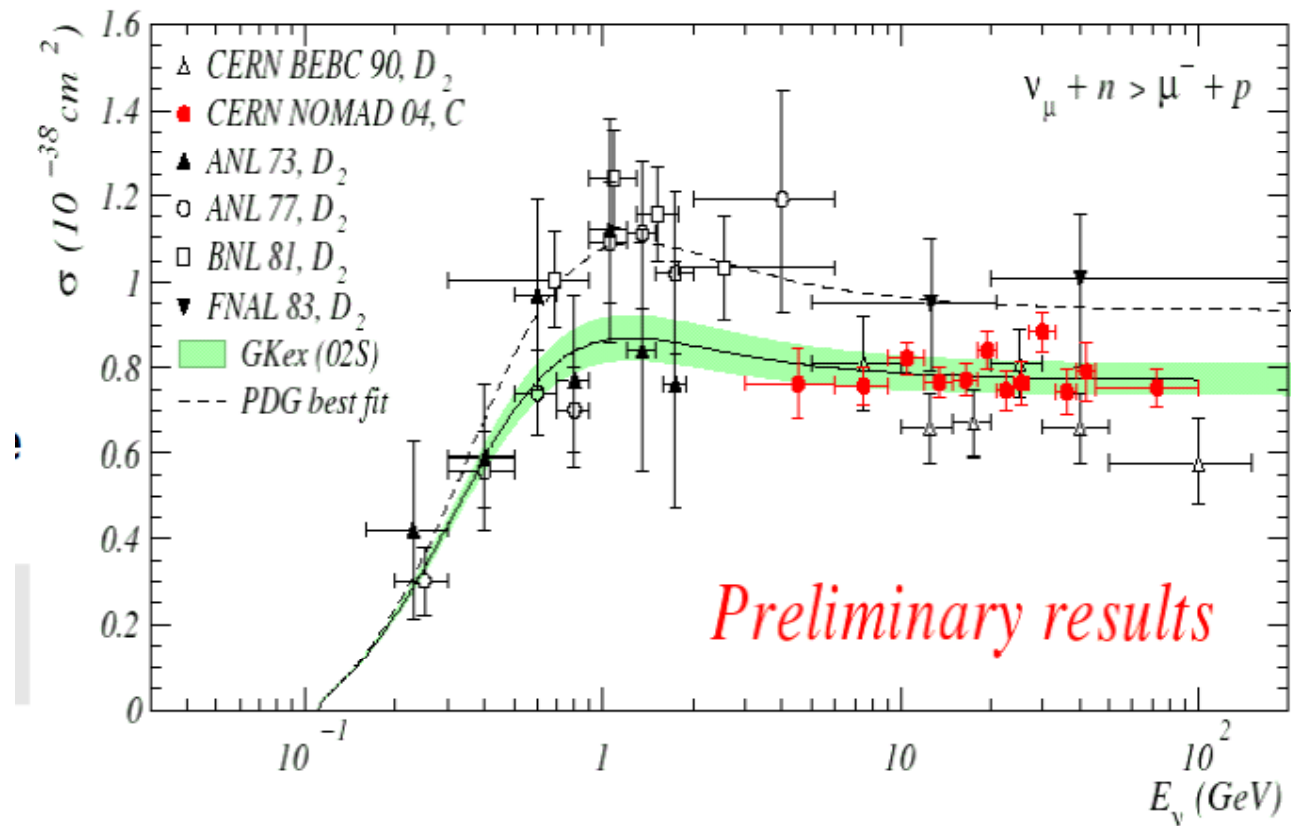
Fig. 5.9. (a) The form factor of the proton as measured in electron-proton scattering. At high q^2 , this is dominated by the distribution of magnetic moment, rather than charge, on the proton. The curve represents the dipole formula (5.28) with $M_V = 0.9$ GeV. (b) The cross-section for the quasi-elastic reactions $\nu_\mu + n \rightarrow \mu^- + p$ (solid circles) and $\bar{\nu}_\mu + p \rightarrow \mu^+ + n$ (open circles). The data comes from measurements in bubble chambers at CERN with freon fillings and from the Argonne National Laboratory (ANL) with deuterium fillings. The curves are for $M_A = M_V = 0.9$ GeV.

Summary of M_A Values



- I wrote that $M_A = 1.05 \pm 0.05$ GeV.
- However, each measurement has large error, and there may be nuclear dependence.

- CC quasi-elastic is one of the most well measured cross section in this energy range. Even so, the precision is NOT great!
 - One of the study items in the next generation experiment.



- CC 1π production: $\nu N \rightarrow \mu N \pi$.
 - The amplitude is sum of $I=1/2$ and $3/2$ processes contributions.

$$A(\nu N \rightarrow \mu N \pi) = \sum_{I_s=1/2,3/2} c_{I_s} A_{I_s}$$

$$A(\nu N \rightarrow \mu^- \Delta^{++} \rightarrow \mu^- p \pi^+) = A_{3/2}$$

$$A(\nu N \rightarrow \mu^- p \pi^0) = \sqrt{2}/3 A_{3/2} - \sqrt{2}/3 A_{1/2}$$

$$A(\nu N \rightarrow \mu^- n \pi^+) = 1/3 A_{3/2} + 2/3 A_{1/2}$$

– $C_{3/2}$ for Δ

$\left \frac{3}{2}, \frac{3}{2} \right\rangle$	$= \pi^+ p$
$\left \frac{3}{2}, \frac{1}{2} \right\rangle$	$= \sqrt{\frac{1}{3}} \pi^+ n + \sqrt{\frac{2}{3}} \pi^0 p$
$\left \frac{3}{2}, -\frac{1}{2} \right\rangle$	$= \sqrt{\frac{2}{3}} \pi^0 n + \sqrt{\frac{1}{3}} \pi^- p$
$\left \frac{3}{2}, -\frac{3}{2} \right\rangle$	$= \pi^- n$

- The scattering matrix element through Δ^{++} is

$$T = \frac{G_F}{2} \langle \Delta | V_\lambda - A_\lambda | N \rangle \bar{\nu}_\mu(k') \gamma^\lambda (1 - \gamma_5) \mu(k)$$

- By introducing form factors,

$$\begin{aligned} \frac{d\sigma}{dt} &\approx \frac{G^2}{24\pi} \frac{s - m_\Delta^2}{s - m_N^2} \left(\frac{m_\Delta + m_N}{m_\Delta} \right)^2 |C_{5^A}(t)|^2 \\ \sigma &= \frac{G^2}{72\pi} |C_{5^A}(t)|^2 \left(\frac{m_A}{m_N} \right)^2 [(m_\Delta + m_N)^2 + m_A^2/2] \end{aligned}$$

- $\sigma \sim 4 \times 10^{-38} \text{ cm}^2$ is good agreement with the $\nu p \rightarrow \mu^- p \pi^+$ experiment for $m_{p\pi} < 1.4 \text{ GeV}$.

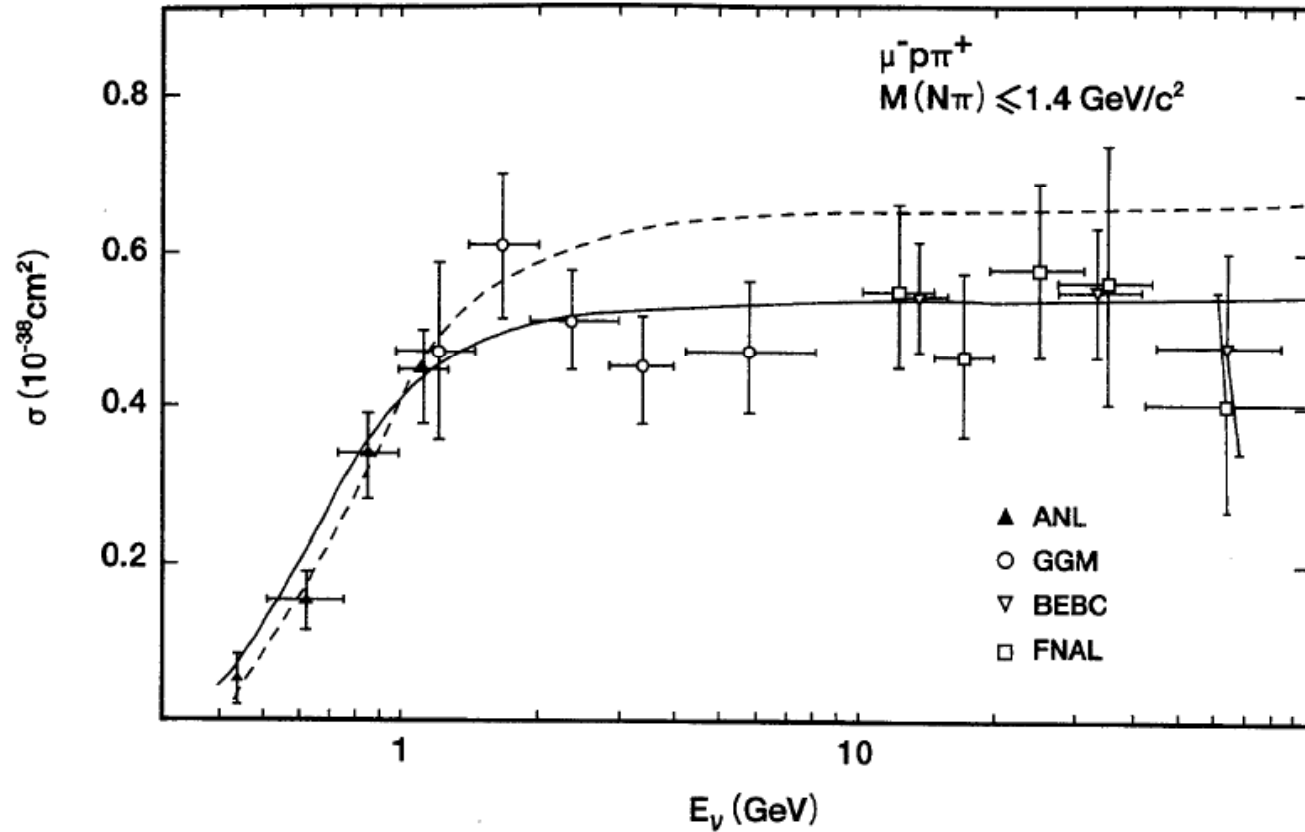


Fig. 3.16. Cross section of $\nu p \rightarrow \mu^- p\pi^+$ as a function of the energy of the neutrino for the final hadron invariant mass of $M(N\pi) \leq 1.4 \text{ GeV}$. The *solid curve* is the prediction of Fogli and Narduli [501], and the *dashed* is that of Rhein and Sehgal [508], compared with data taken from BEBC [502], FNAL [503], ANL [504], and Gargamelle (GGM) [505].

- For Δ resonance, we have 14 final state overall
(6CC and 8NC)

CC

$$\begin{array}{ll}
 \nu_\mu p \rightarrow \mu^- \Delta^{++} & \Delta^{++} \rightarrow p\pi^+ \\
 \nu_\mu n \rightarrow \mu^- \Delta^+ & \Delta^+ \rightarrow p\pi^0, \Delta^+ \rightarrow n\pi^+ \\
 \bar{\nu}_\mu p \rightarrow \mu^+ \Delta^0 & \Delta^0 \rightarrow n\pi^0, \Delta^0 \rightarrow p\pi^- \\
 \bar{\nu}_\mu n \rightarrow \mu^+ \Delta^- & \Delta^- \rightarrow n\pi^- \\
 \end{array}$$

NC

$$\begin{array}{ll}
 \nu_\mu p \rightarrow \nu_\mu \Delta^+ & \Delta^+ \rightarrow p\pi^0, \Delta^+ \rightarrow n\pi^+ \\
 \nu_\mu n \rightarrow \nu_\mu \Delta^0 & \Delta^0 \rightarrow n\pi^0, \Delta^0 \rightarrow p\pi^- \\
 \bar{\nu}_\mu p \rightarrow \bar{\nu}_\mu \Delta^+ & \Delta^+ \rightarrow p\pi^0, \Delta^0 \rightarrow n\pi^+ \\
 \bar{\nu}_\mu n \rightarrow \bar{\nu}_\mu \Delta^0 & \Delta^0 \rightarrow n\pi^0, \Delta^0 \rightarrow p\pi^- \\
 \end{array}$$

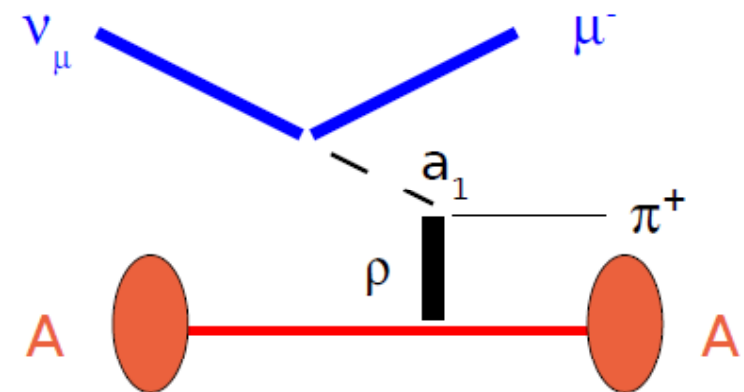
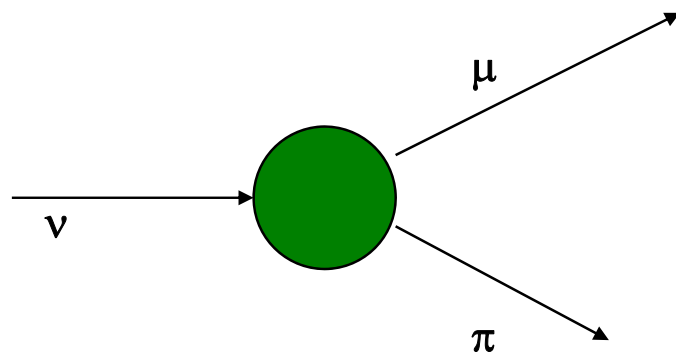
- For other π production process, we must consider other Δ resonance including off-shell Δ 's.
 - What is the effect of $A_{1/2}$?
 - $R = |A_{1/2}| / |A_{3/2}| = 0.68 \pm 0.04$
 - The experimental result is consistent with a resonant $I=3/2$ amplitude in the presence of a large non-resonant $I=1/2$ background.
 - Experimental results:

$$\frac{\sigma(\mu^- n \pi^+)}{\sigma(\mu^- p \pi^0)} = \frac{1}{2} \quad \text{for } A_{3/2}$$

but experimental result is 0.96 ± 0.12

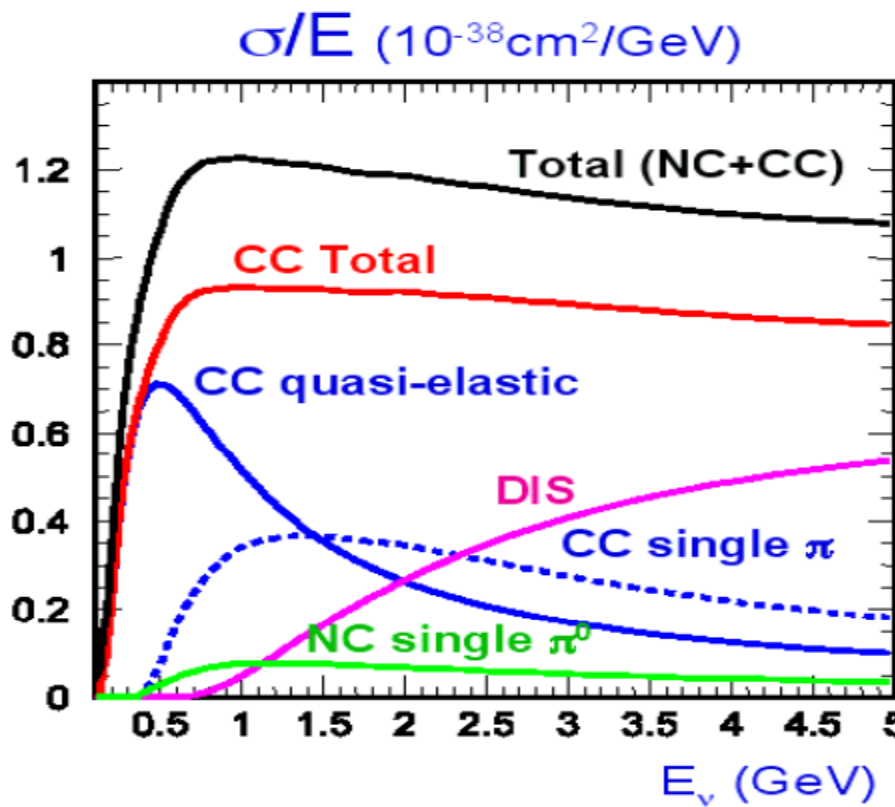
Coherent π production

CC-coherent π ($\nu+A \rightarrow \mu+A+\pi$)



Neutrino interacts coherently with nucleons bound in the nucleus, producing pion.

- may be too details as a lecture.



- DIS (Deep Inelastic Scattering) will be discussed in the next chapter since it is a dominant cross section at the high energy.

4. Cross Sections of 10~100GeV neutrinos

- Deep inelastic scattering
 - Scattering with a quark in a nucleus
Example: a proton with the ν_μ beam
 - $\nu_\mu + d \rightarrow \mu^- + u$ scattering
$$\frac{d^2\sigma}{dxdy} \sigma(\nu_\mu d \rightarrow \mu^- u) = \frac{G^2 \cos^2 \theta_C}{\pi} xs$$
 - x (Feynman x) is the momentum fraction of the quark in the proton.
 - Anti-quarks exist in a proton as a sea quark.

$$\frac{d^2\sigma}{dxdy} \sigma(\nu_\mu \bar{u} \rightarrow \mu^- \bar{d}) = \frac{G^2 \cos^2 \theta_C}{\pi} xs (1 - y)^2$$

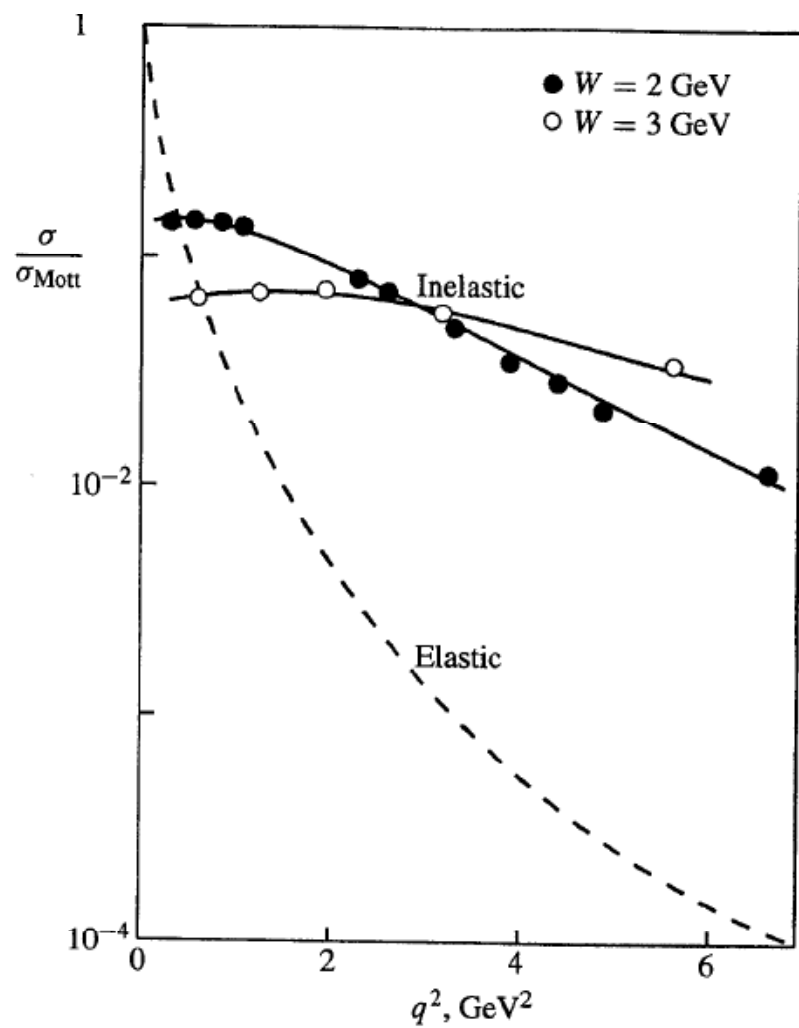


Fig. 5.11. Early SLAC measurements of the inelastic electron-proton scattering cross-section divided by the Mott (pointlike) cross-section, for two values of the invariant mass W of the hadronic final state. The ratio is seen to be only weakly q^2 -dependent, in contrast with the strong q^2 dependence of the elastic scattering process, taken from Figure 5.9.

- In the proton, we define the quark distribution function: $u(x)$, $d(x)$, $s(x)$, The cross section with a proton is

$$\frac{d^2\sigma}{dxdy} \sigma (\nu_\mu p) = \frac{G^2 \cos^2 \theta_C}{\pi} xs \left[d(x) + \bar{u}(x)(1-y)^2 \right]$$

- In the case of neutron, by using the isospin symmetry ($d^n(x)=u^p(x)$),

$$\frac{d^2\sigma}{dxdy} \sigma (\nu_\mu n) = \frac{G^2 \cos^2 \theta_C}{\pi} xs \left[u(x) + \bar{d}(x)(1-y)^2 \right]$$

- In the case of isoscalar target ($\sum n = \sum p$)

$$\frac{d^2\sigma}{dxdy} \sigma (\nu_\mu N) = \frac{G^2 \cos^2 \theta_C}{2\pi} xs \left\{ [u(x) + d(x)] + [\bar{u}(x) + \bar{d}(x)](1-y)^2 \right\}$$

- For anti-neutrinos,

$$\frac{d^2\sigma}{dxdy} \sigma (\bar{\nu}_\mu N) = \frac{G^2 \cos^2 \theta_C}{2\pi} xs \left\{ [u(x) + d(x)](1-y)^2 + [\bar{u}(x) + \bar{d}(x)] \right\}$$

$$Q = \int x [u(x) + d(x)] dx , \quad \bar{Q} = \int x [\bar{u}(x) + \bar{d}(x)] dx ,$$

$$\sigma(\nu N) = \frac{G^2 \cos^2 \theta_C m_p E}{\pi} \left(Q + \frac{1}{3} \bar{Q} \right)$$

$$\sigma(\bar{\nu} N) = \frac{G^2 \cos^2 \theta_C m_p E}{\pi} \left(\bar{Q} + \frac{1}{3} Q \right)$$

$$\sigma(\nu N) \approx 2 \times \sigma(\bar{\nu} N)$$

$$\Rightarrow \bar{Q}/Q \approx 0.15$$

- This example is CC current.

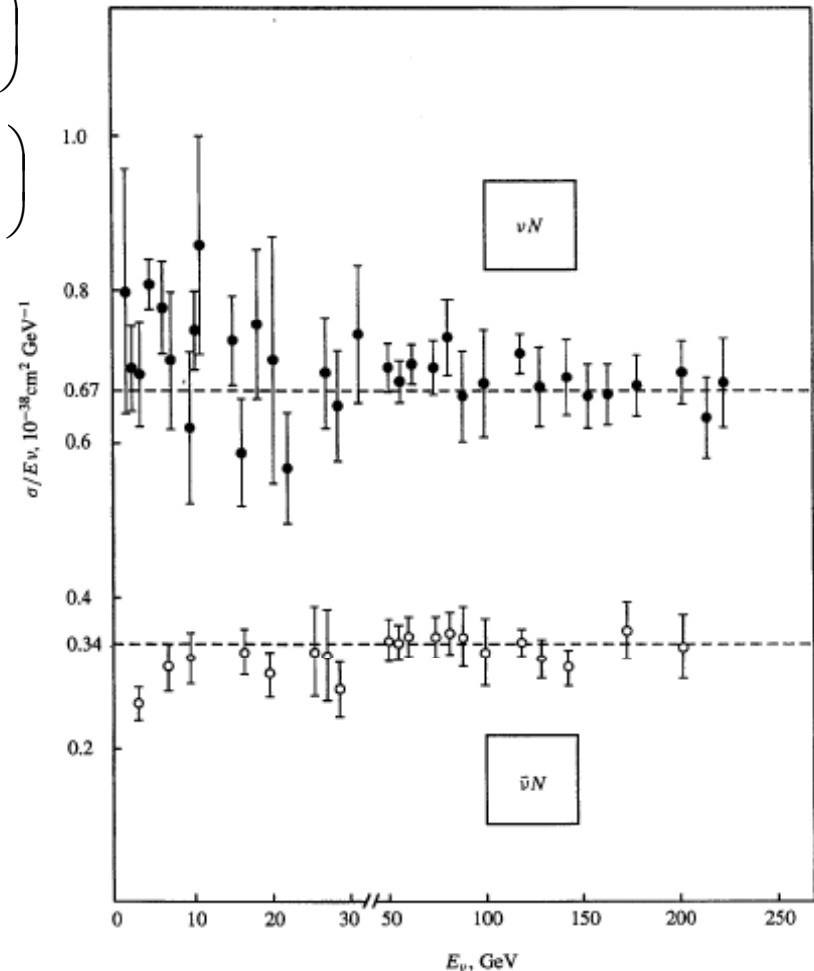


Fig. 5.13. Neutrino and antineutrino cross-sections on nucleons. The ratio σ/E_ν is plotted as a function of energy and is indeed a constant, as predicted in (5.45) and (5.46).

- NC current:

$$\left(\frac{d^2 \sigma}{dxdy} \right)_{\nu N \rightarrow \nu N} = \frac{G^2 s}{4 \pi} \rho \left[x q_1(x) + x (1 - y)^2 \bar{q}_1(x) \right]$$

$$q_1(x) = 4 \left[g_L^2(u) + g_L^2(d) \right] q(x) + 4 \left[g_R^2(u) + g_R^2(d) \right] \bar{q}(x)$$

$$\bar{q}_1(x) = 4 \left[g_L^2(u) + g_L^2(d) \right] \bar{q}(x) + 4 \left[g_R^2(u) + g_R^2(d) \right] q(x)$$

- What is $g_L(u)$, $g_R(u)$, $g_L(d)$, $g_R(d)$?

$$-i \frac{g}{\cos\theta_W} (J_\mu^3 - \sin^2\theta_W J_\mu^{EM}) Z^\mu$$

	g_L	g_R
e, μ, τ	-½+sin ² θ _W	sin ² θ _W
v	½	0
u,c,t	½-2/3*sin ² θ _W	-2/3*sin ² θ _W
d,s,b	-½+1/3*sin ² θ _W	1/3*sin ² θ _W

$$\begin{aligned}
R(\nu N) &= \frac{\sigma^{NC}(\nu N \rightarrow \nu + X)}{\sigma^{CC}(\nu N \rightarrow \mu + X)} \\
&= [1/2 - \sin^2 \theta_w + 5/9 (1+r) \sin^4 \theta_w] \rho \\
R(\bar{\nu} N) &= \frac{\sigma^{NC}(\bar{\nu} N \rightarrow \bar{\nu} + X)}{\sigma^{CC}(\bar{\nu} N \rightarrow \mu + X)} \\
&= [1/2 - \sin^2 \theta_w + 5/9 (1+1/r) \sin^4 \theta_w] \rho \\
r &= \frac{\sigma(\bar{\nu} N \rightarrow \mu^+ + X)}{\sigma(\nu N \rightarrow \mu^- + X)} = \frac{1/3 + \overline{Q}/Q}{1 + \overline{Q}/3Q}
\end{aligned}$$

- FNAL NuTeV experiment measured this quantities.

NuTeV results on R^ν and $R^{\bar{\nu}}$

- NuTeV result:

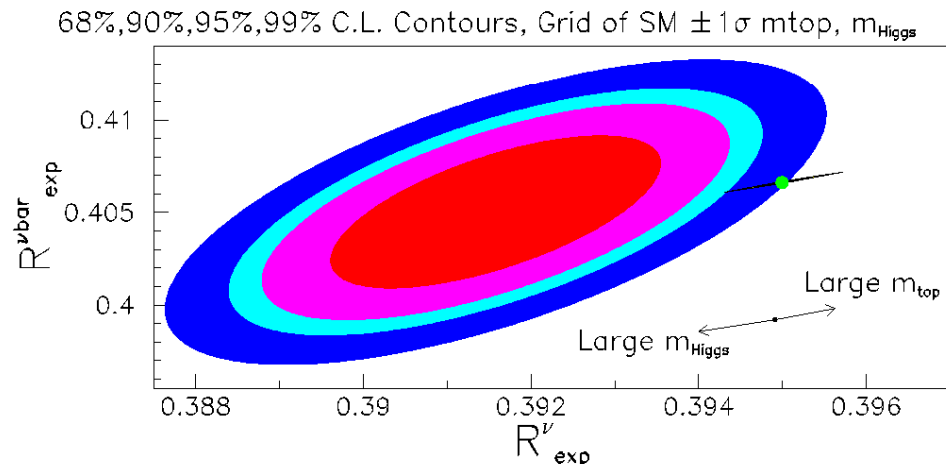
$$\begin{aligned}\sin^2 \theta_W^{(on-shell)} &= 0.2277 \pm 0.0013(stat.) \pm 0.0009(syst.) \\ &= 0.2277 \pm 0.0016\end{aligned}$$

- Standard model fit (LEPEWWG): 0.2227 ± 0.00037

A 3σ discrepancy...

$R_\text{exp}^\nu = 0.3916 \pm 0.0013$
 $(SM : 0.3950) \Leftarrow 3\sigma \text{ difference}$

$R_\text{exp}^{\bar{\nu}} = 0.4050 \pm 0.0027$
 $(SM : 0.4066) \Leftarrow \text{Good agreement}$



5. *Cross Sections of >TeV neutrinos*

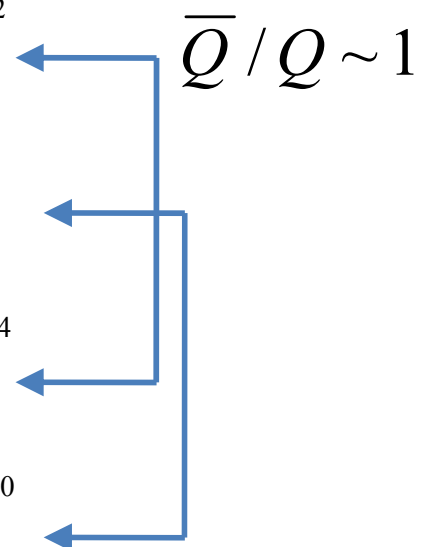
- Neutrinos are an important particle to search for astrophysical sources.
 - Example: ICE-Cube experiment.
 - The energy of neutrino is much higher than that available by an accelerator.
 - Basic interaction is DIS with some corrections.
 - $G_F^2 \rightarrow G_F^2 \frac{1}{(1 - q^2/m_W^2)^2} = G_F^2 \frac{1}{(1 - 2m_N E_\nu xy/m_W^2)^2}$
 - Small x (sea quark contribution) is getting important.

$$\sigma_{CC} (\nu N) \approx 2.69 \times 10^{-36} \text{ cm}^2 \left(\frac{E_\nu}{1 \text{ GeV}} \right)^{0.402}$$

$$\sigma_{NC} (\nu N) \approx 1.06 \times 10^{-36} \text{ cm}^2 \left(\frac{E_\nu}{1 \text{ GeV}} \right)^{0.408}$$

$$\sigma_{CC} (\bar{\nu} N) \approx 2.53 \times 10^{-36} \text{ cm}^2 \left(\frac{E_\nu}{1 \text{ GeV}} \right)^{0.404}$$

$$\sigma_{NC} (\bar{\nu} N) \approx 0.98 \times 10^{-36} \text{ cm}^2 \left(\frac{E_\nu}{1 \text{ GeV}} \right)^{0.410}$$

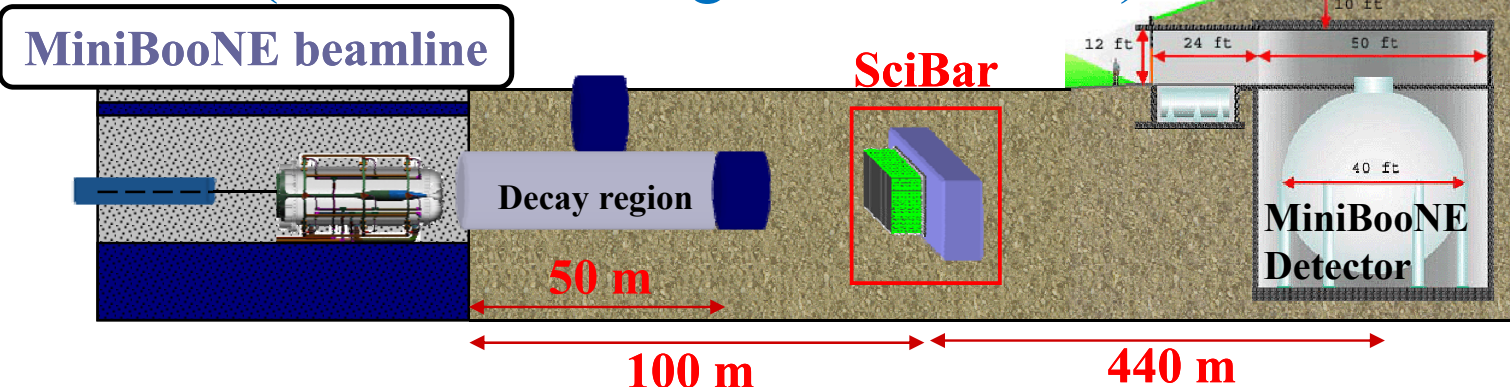


HOMEWORK: For an example, how long is the interaction length of 100TeV neutrino in ice?

6. Experiments for neutrino cross sections

- Neutrino detectors in the short baseline oscillation experiment
 - NuTeV, NOMAD, CHORUS, MiniBooNE
- Near neutrino detectors in the long baseline oscillation experiment.
 - K2K, MINOS, T2K, NOvA
- Dedicated experiments to measure the neutrino cross section
 - SciBooNE, MINERvA
 - vSNS
 - study the cross section of $\sim O(10\text{MeV})$ for Supernova detection.

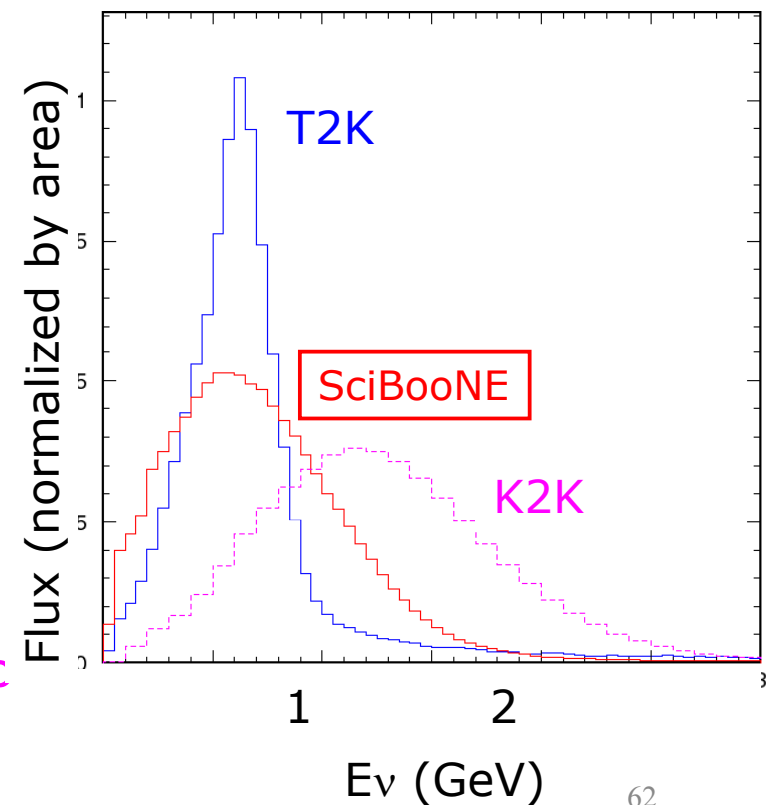
SciBooNE (start data taking in June 2007)



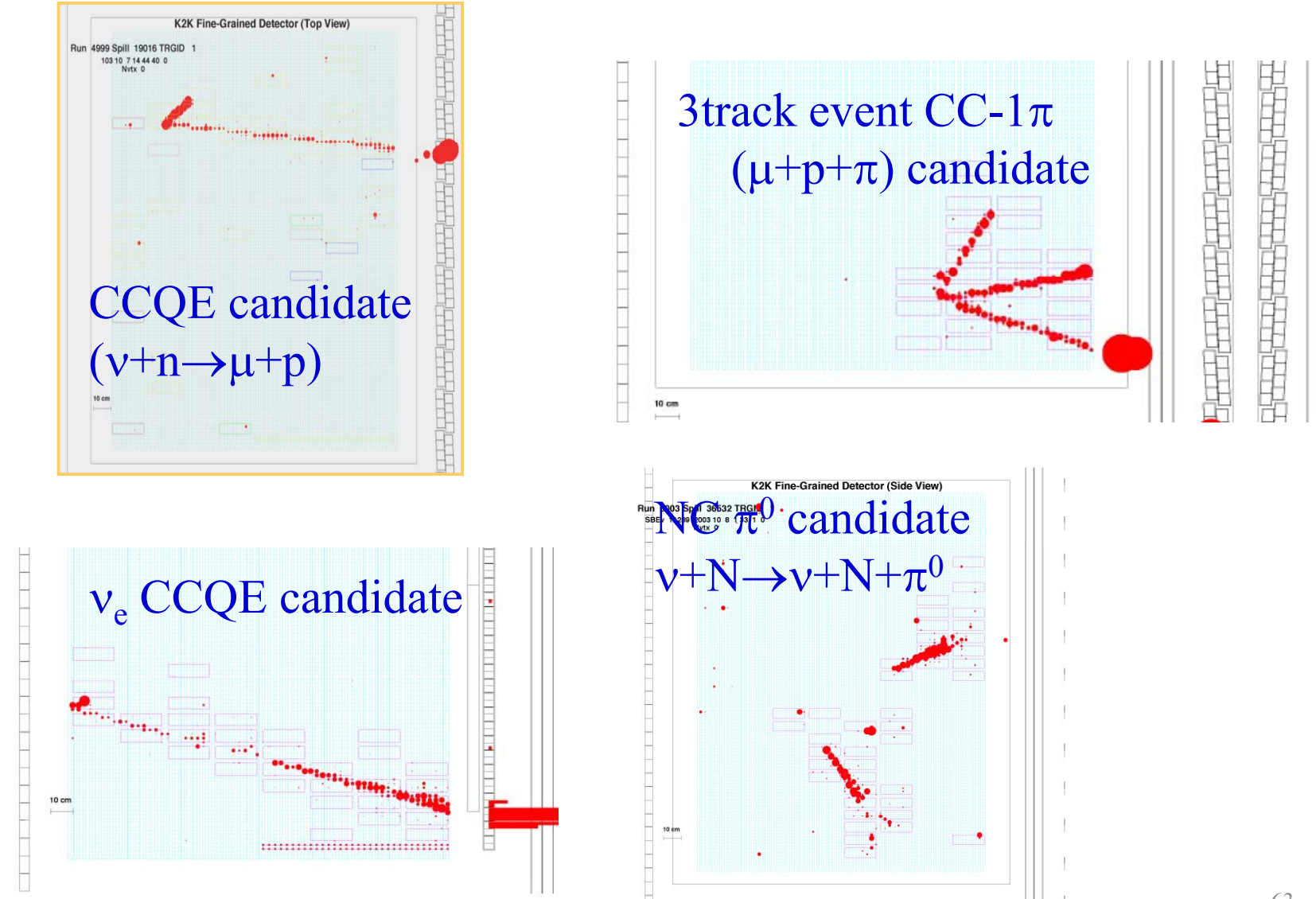
- Precision study of neutrino cross sections for T2K.
- Anti-neutrinos
 - Unexplored physics territory and important for CP study in T2K-II.

K2K-SciBar + FNAL-BNB

- Well developed Detector
- Most intense low energy neutrino beam.

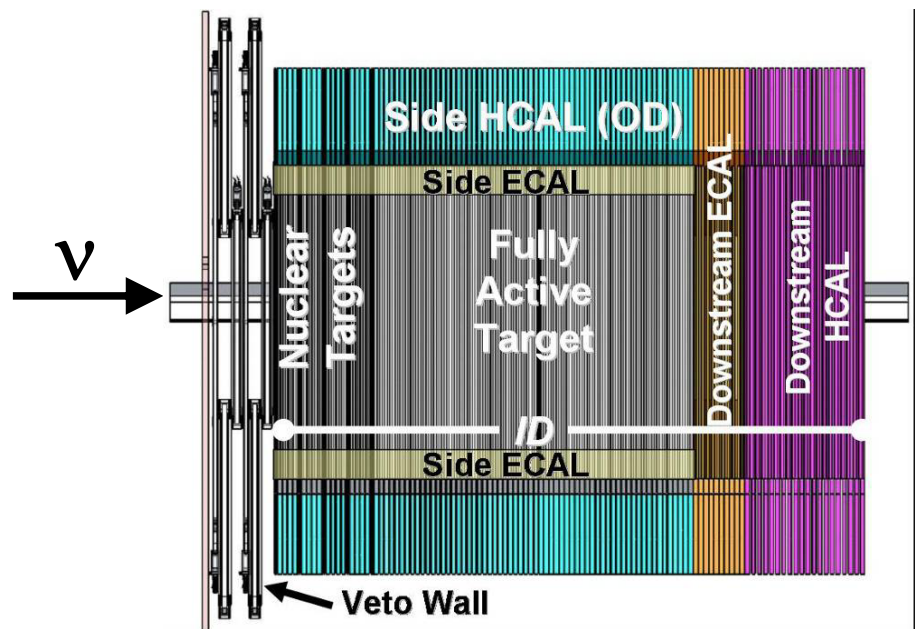
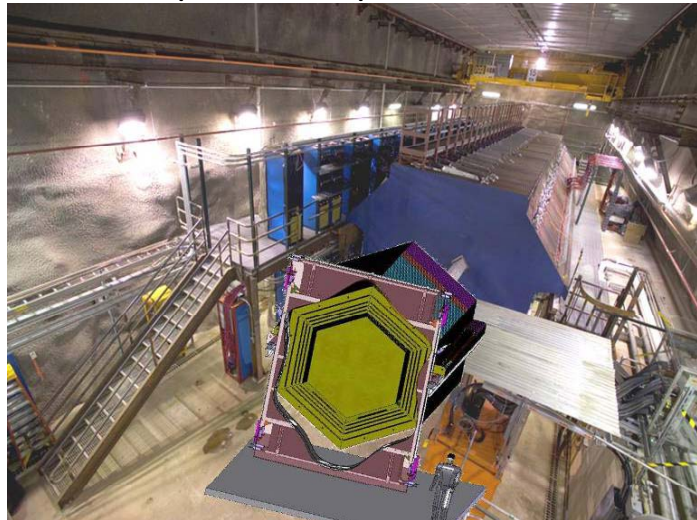


SciBar detector event display in K2K

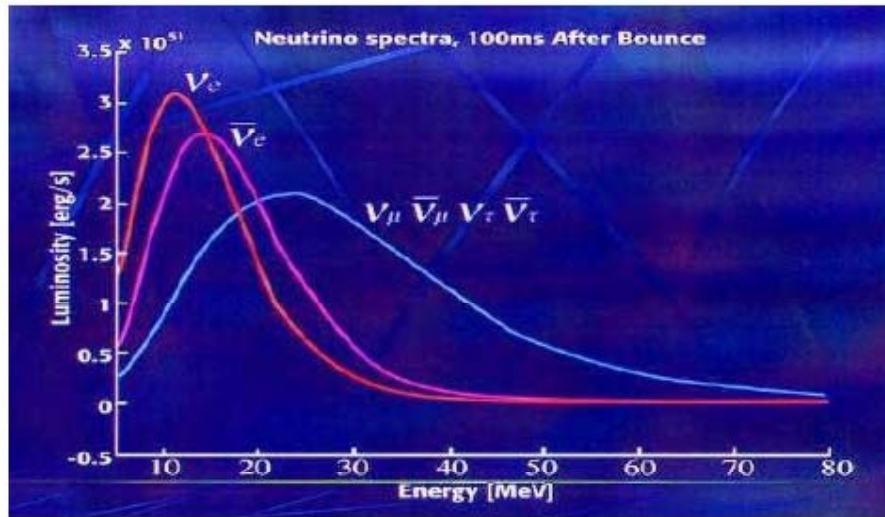


MINERvA at NuMI (start in 2009)

- Need a high granularity detector (like SciBar) but in a higher energy beam and with improved containment of γ , π^\pm , μ



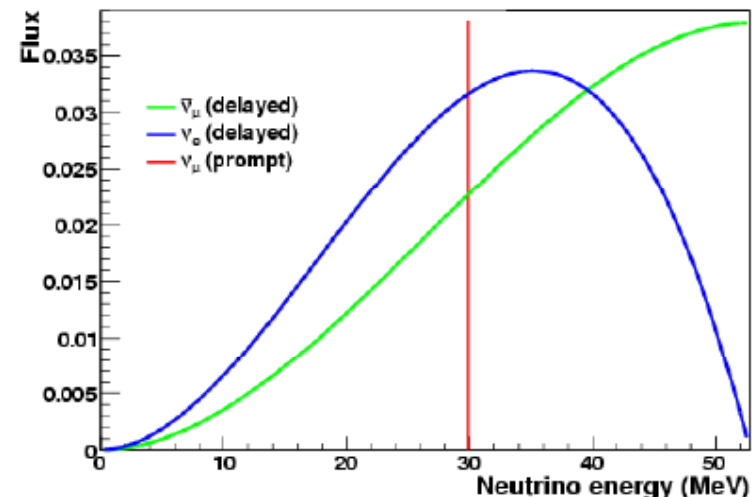
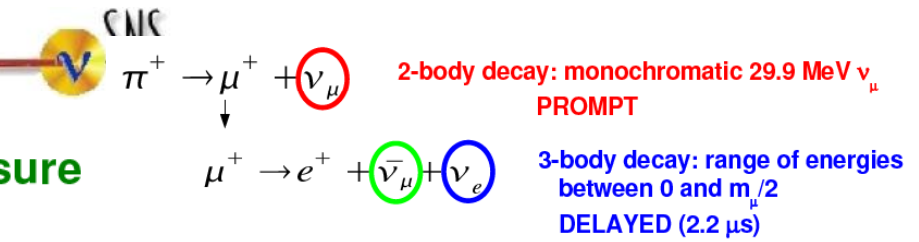
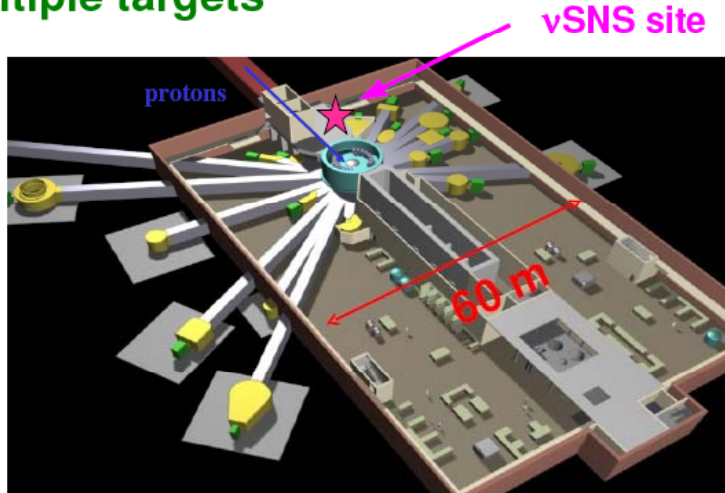
- MINERvA at NuMI
 - “chewy center” (active target)
 - with a crunchy shell of muon, hadron and EM absorbers



**Study
CC and NC
interactions
with various
nuclei,
in few to 10's
of MeV range**

NuSNS (Neutrinos at the SNS)

A neutrino facility with capability to measure multiple targets



7. Summary

- Understanding of neutrino cross section is a good exercise to review the standard model.
- In reality, the reliable estimation is not easy because of the nuclear (and nucleon?) structure.
 - Experimental Inputs and model buildings are essential!
- The next generation *precision* oscillation experiments request the precise information of neutrino cross sections.
 - Including the final state kinematics (although I did not fully cover this topics in the lecture).
-

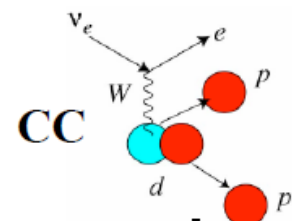
Play together with neutrinos!

Reference materials

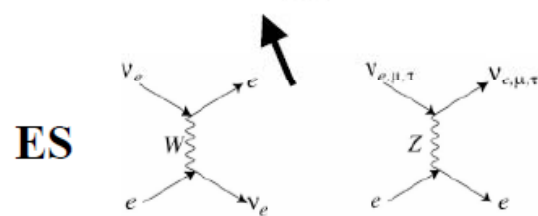
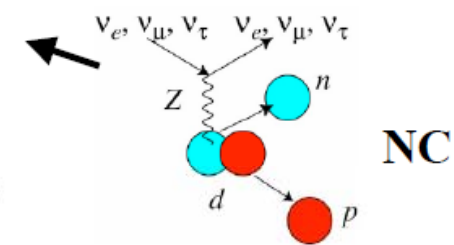
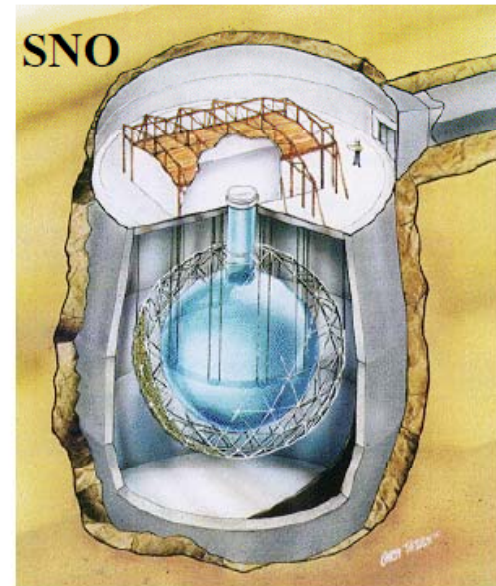
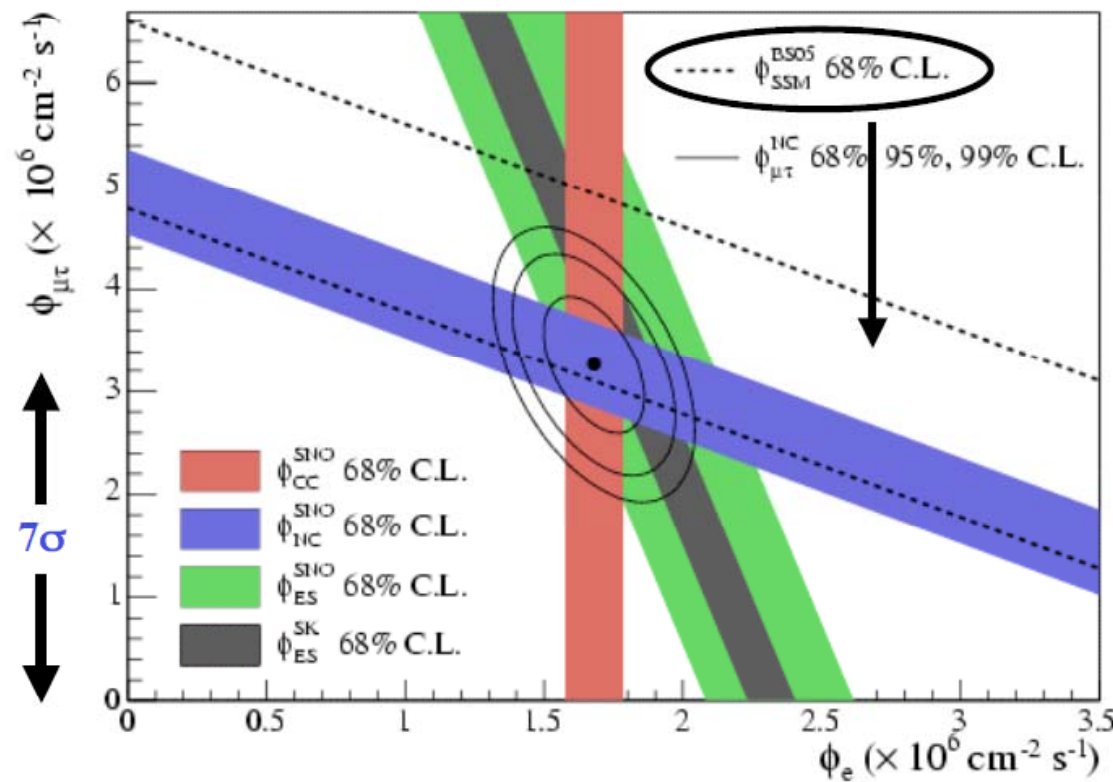
Neutrino Experiments

- KamLAND, Super-K, SNO, Borexino, GNO, Homestake, one more
- LSND, Karmen
- K2K, T2K, Super-K, MINOS, Soudan2, MACRO, MiniBooNE
- NuTeV, CCFR, OPERA, CHORUS, NOMAD
- SciBooNE, MINERnA

SNO



SNO Collaboration, PRC 72, 055502 (2005)
391 Days of Dissolved Salt Data



1. Introduction

Neutrino Oscillation Experiments.

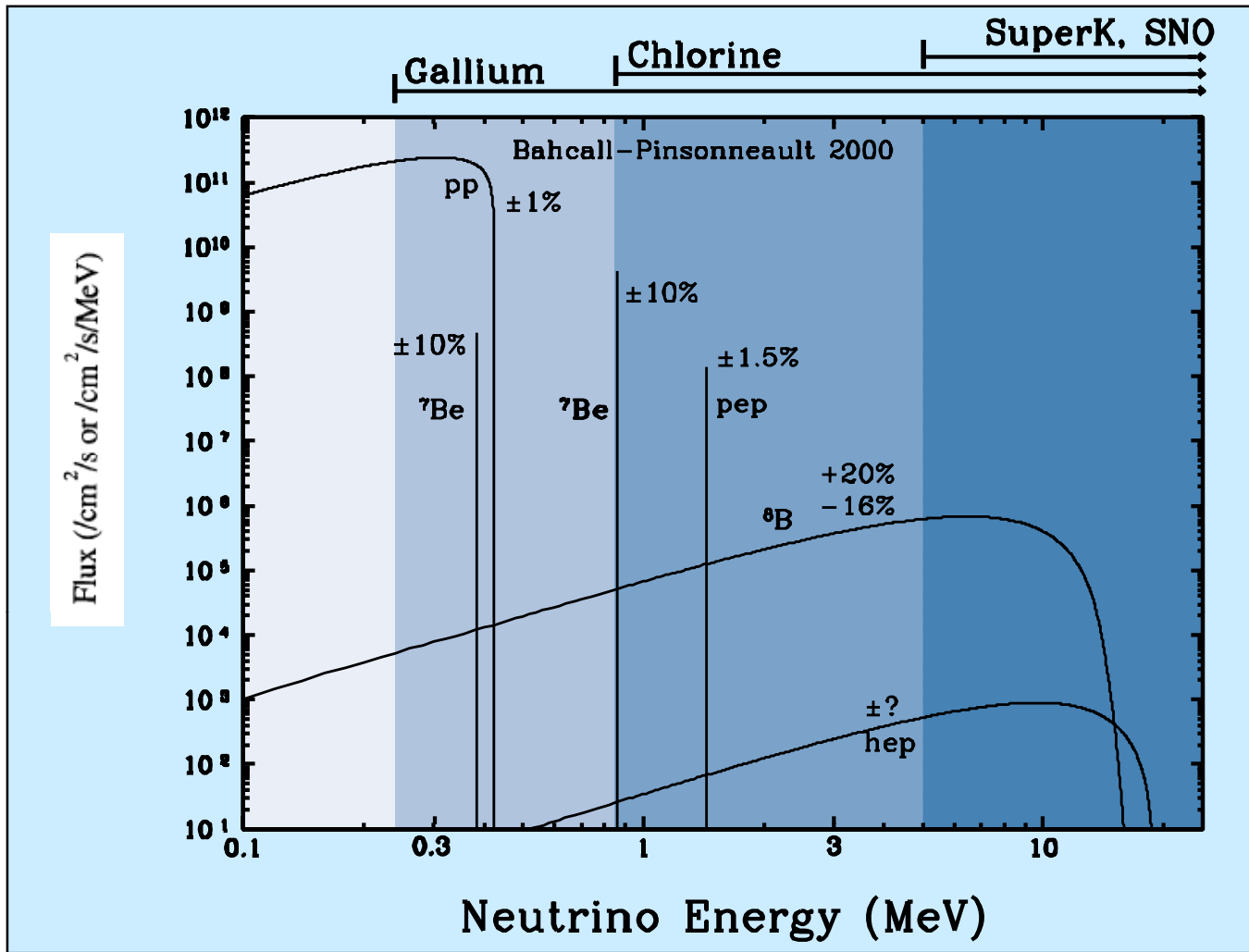
- Experimental Condition:
 - Solar Neutrinos (ν_e)
 $E_\nu \sim 0.1 \sim 15 \text{ MeV}$, $L \sim 1.5 \times 10^8 \text{ km}$, $\Delta m^2 \sim > 10^{-11} \text{ eV}^2$, $\sigma_\nu \sim 10^{-43} \text{ cm}^2$.
 - Reactor Neutrinos ($\bar{\nu}_e$)
 $E_\nu \sim 1 \sim 9 \text{ MeV}$, $L \sim 1 \sim 100 \text{ km}$, $\Delta m^2 \sim > 10^{-5} \text{ eV}^2$, $\sigma_\nu \sim 10^{-41} \text{ cm}^2$.
 - Atmospheric Neutrinos ($\nu_e, \bar{\nu}_e, \nu_\mu, \bar{\nu}_\mu$)
 $E_\nu \sim 20 \sim > 10^5 \text{ MeV}$, $L \sim 10 \sim 1 \times 10^4 \text{ km}$, $\Delta m^2 \sim > 10^{-4} \text{ eV}^2$, $\sigma_\nu \sim 10^{-42} \sim 10^{-36} \text{ cm}^2$.
 - Accelerator Neutrinos ($\nu_e, \bar{\nu}_e, \nu_\mu, \bar{\nu}_\mu$)
 $E_\nu \sim 20 \sim 10^5 \text{ MeV}$, $L \sim 0.01 \sim 1000 \text{ km}$, $\Delta m^2 \sim > 10^{-3} \text{ eV}^2$, $\sigma_\nu \sim 10^{-42} \sim 10^{-36} \text{ cm}^2$.

- Neutrino Targets:
 - Solar Neutrinos:
 - Gallex(GNO), SAGE, Homestake, Kamiokande, Super-K, SNO
 - Ga, Cl, H₂O, D₂O and e⁻,
 - Reactor Neutrinos:
 - CHOOZ, KamLAND
 - C (Carbon),
 - Atmospheric Neutrinos:
 - Soudan2, Kamioaknde, Super-K, MINOS, MACRO
 - Fe, H₂O , CH
 - Accelerator Neutrinos:
 - LSND, MiniBooNE, K2K, MINOS, OPERA, CCFR, CHORUS, NOMAD
 - Carbon, H, Fe, H₂O, and other Nucleus

Neutrino Flux

Solar Neutrino Flux

Plot adapted from <http://www.sns.ias.edu/~jinb/>



Reactor Neutrinos

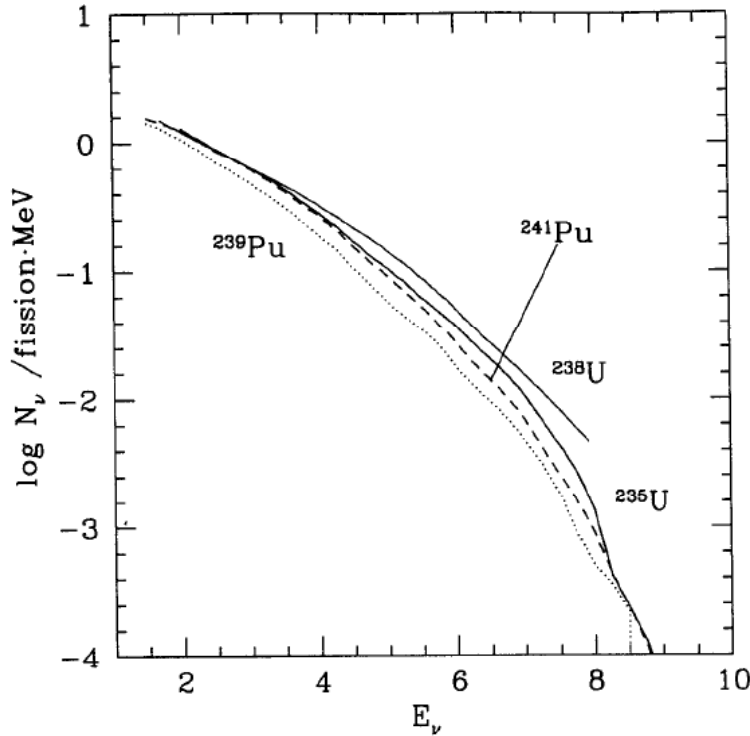


Fig. 4.2. Neutrino spectra from fission of ^{235}U , ^{239}Pu , ^{241}Pu (measured), and ^{238}U (calculated).

- KamLAND Flux: $2 \times 10^6 \text{ cm}^{-2} \text{s}^{-1}$
 - 70GW reactors at 100 – 250 km away

Accelerator neutrino flux

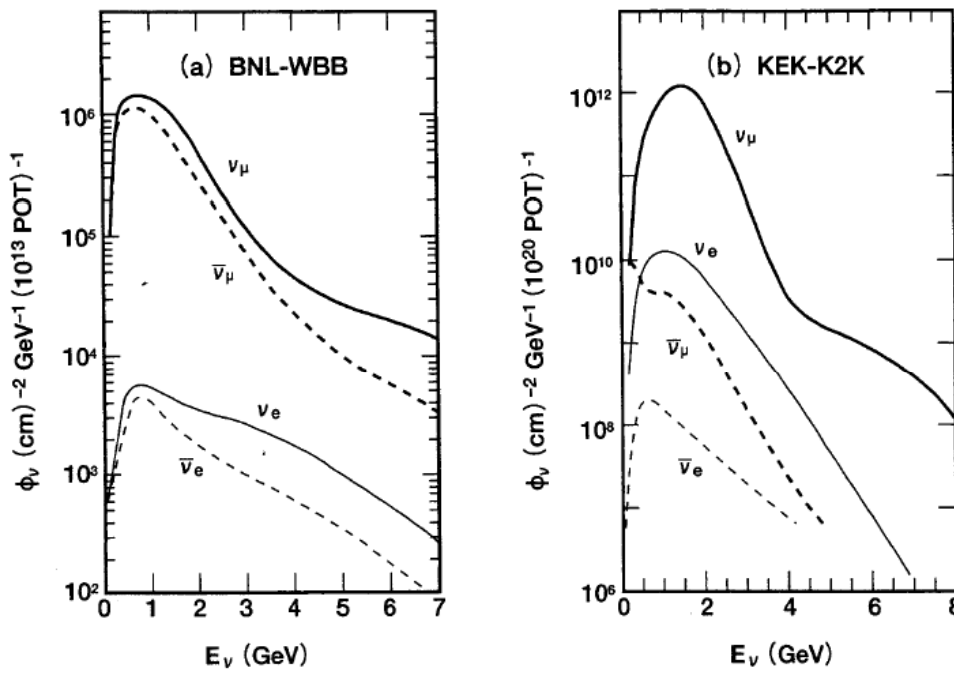


Fig. 4.4. (a) Neutrino flux in the Brookhaven AGS wide-band neutrino beam produced from 28.3-GeV protons on a sapphire (Al_2O_3) target with two horns ($12 \text{kV} \times 250 \text{kA}$) which enhance alternatively the neutrino or antineutrino flux. The curve shows the flux at the detector located 110 m away from the second horn with 10^{13} protons incident on target (POT). Data taken from [551]. (b) Neutrino flux produced by the KEK 12 GeV PS, used for the K2K long baseline neutrino oscillation experiment at Kamioka. The curve shows the flux at the front detector, which is located at a distance of 300 m from the second horn (operated at 250 kA) which focuses only positively charged particles. 10^{20} POT are the goal number of accumulated protons in the K2K experiment. Data taken from [558].

Atmospheric neutrino flux

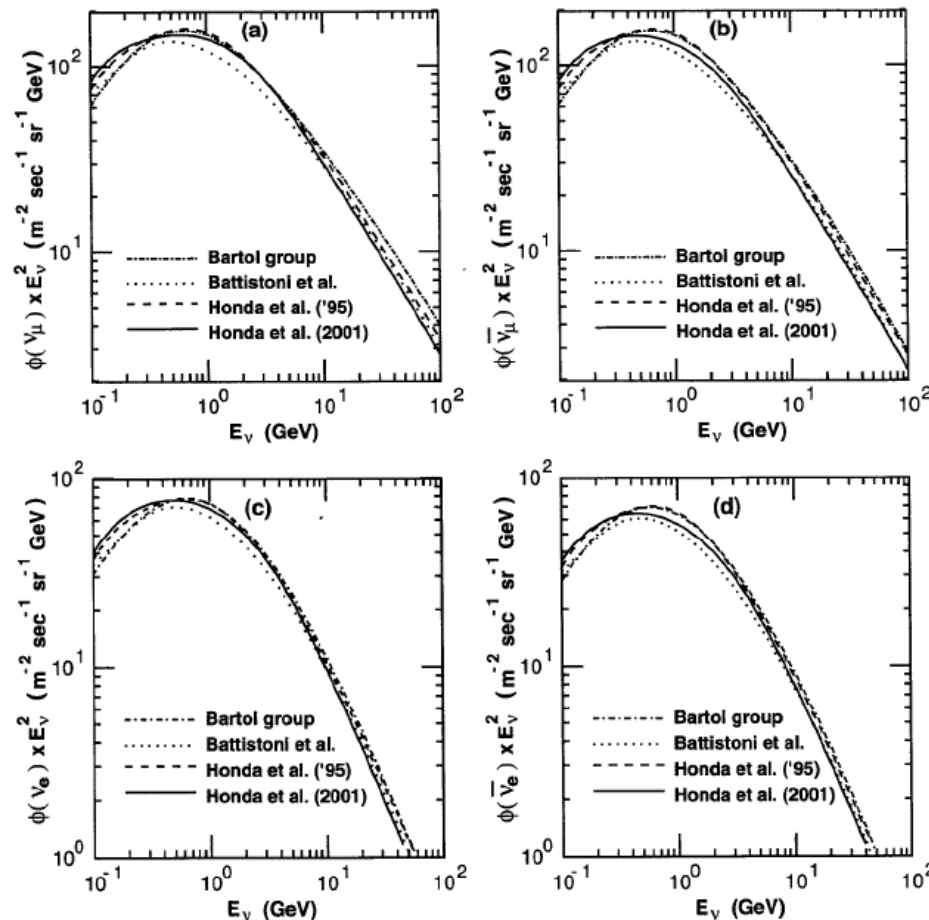


Fig. 4.10. Comparison of the atmospheric neutrino fluxes of BGS [563]/AGLS [564] (Bartol group), Battistoni et al. [572], HKKM [565] (Honda et al. 1995), and Honda et al. 2001 [610]: (a) ν_μ flux, (b) $\bar{\nu}_\mu$ flux, (c) ν_e flux, and (d) $\bar{\nu}_e$ flux.

Cosmic Ray flux

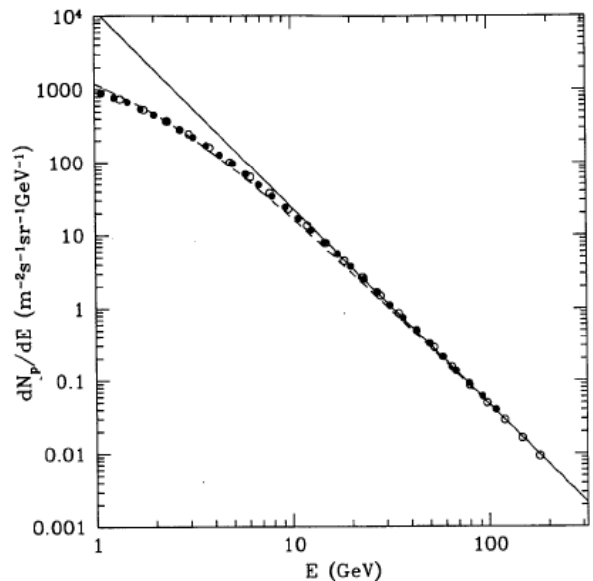


Fig. 4.5. Cosmic-ray proton flux measured by BESS (solid circles) and AMS (open circles). The solid curve represents (4.7). The dashed curve that closely matches the data points is the same spectrum but modulated by the solar wind according to the Gleeson–Axford formula (4.9) with $\phi = 750$ MeV.

Features of atmospheric neutrino flux.

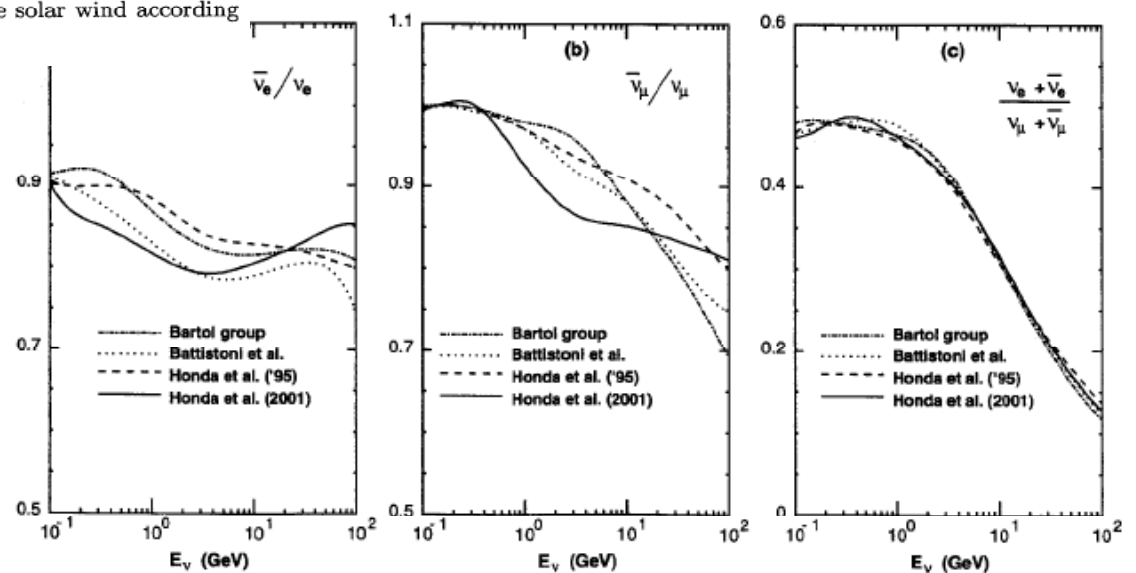


Fig. 4.11. Comparison of the atmospheric neutrino flux calculations for ratios (a) $\bar{\nu}_e/\nu_e$, (b) $\bar{\nu}_\mu/\nu_\mu$, and (c) $(\nu_e + \bar{\nu}_e)/(\nu_\mu + \bar{\nu}_\mu)$. See Fig. 4.10 for references.

Supernova neutrino flux

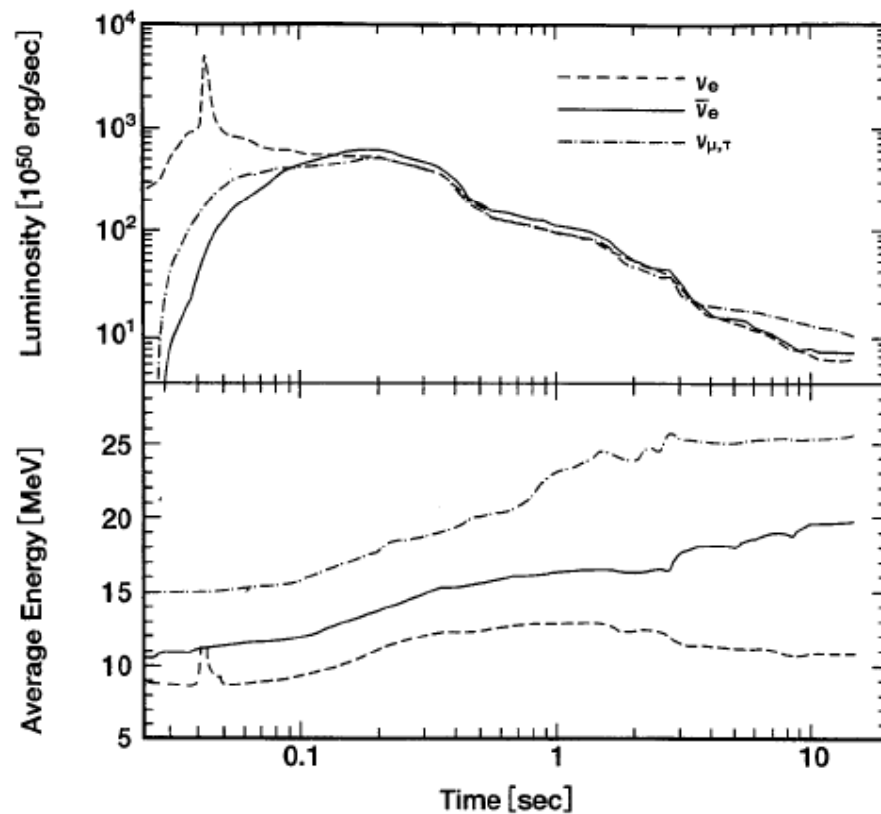


Fig. 4.21. Typical neutrino fluxes from a stellar core collapse, as calculated by Wilson and collaborators. The upper panel shows the luminosity, and lower panel shows the mean energy. $\nu_{\mu,\tau}$ stands for each of ν_μ , ν_τ and their antiparticles. After Totani et al. [784].

Geo-neutrino flux

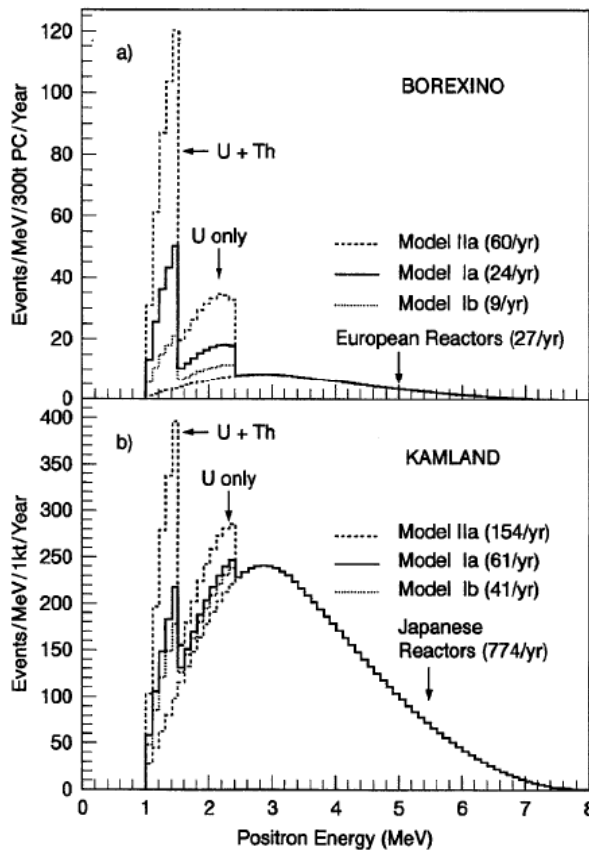


Fig. 4.27. Antineutrino spectrum from ^{238}U and ^{232}Th deposited in Earth's crust, expected in Borexino and KamLAND neutrino detectors. The three curves show different models: Ia and Ib correspond to two different models with the estimated crustal abundance of U/Th [914]; II assumes a full 40 TW ascribed to U/Th radioactivity. Model a employs an estimated distribution of crustal U/Th [914], and b assumes a uniform distribution in the crust. After [913].